





# Impact of heat treatment on the surface quality of electropolished WE43 alloy

Jessica Kloiber<sup>a,b,\*</sup> , Ulrich Schultheiß<sup>a,c</sup>, Helga Hornberger<sup>a,b,c</sup> 

<sup>a</sup> Biomaterials Laboratory, Ostbayerische Technische Hochschule (OTH) Regensburg, Seybothstraße 2, Regensburg 93053, Germany

<sup>b</sup> Regensburg Center of Biomedical Engineering (RCBE), Ostbayerische Technische Hochschule (OTH) Regensburg, Seybothstraße 2, Regensburg 93053, Germany

<sup>c</sup> Analytics Center, Ostbayerische Technische Hochschule (OTH) Regensburg, Seybothstraße 2, Regensburg 93053, Germany

## ARTICLE INFO

### Keywords:

Magnesium  
WE43  
Electropolishing  
Heat treatment  
Secondary phases  
Surface

## ABSTRACT

In this study, the Mg alloy WE43 was solution annealed and precipitation hardened prior to electropolishing to evaluate the effects of different microstructures on the electropolishing result. While coarsely distributed precipitates led to surfaces showing wavy structures and dents after electropolishing, a uniform microstructure resulted in an even finish of the surface. The homogenization and refinement of the microstructure by heat treatment is a method to ensure improved electropolished surfaces of Mg materials.

## 1. Introduction

The high specific strength and good castability of Mg rare earths (RE) alloys make them one of the most promising lightweight materials in a variety of engineering applications [1]. By using specific selected RE metals, the Mg-alloy WE43 is of great interest for biodegradable implants because it shows good biocompatibility, appropriate mechanical properties and adequate corrosion stability [2].

There are many methods to improve the corrosion resistance of Mg materials, including alloying, processing, surface modification, etc. [3–5]. Electropolishing developed into a promising surface treatment, as the degradation behavior can be optimized by levelling the surface and forming a more stable oxide layer [6–8]. However, although electropolishing of steel is well known, studies about electropolishing of Mg materials are very rare. As we have seen in our previous study [7], local property changes in the microstructure are limiting the quality level of surface treatment and cause irregularities on the electropolished surface which can be decisive for subsequent corrosion processes. Local property changes are caused by secondary phases which can vary in shape, size, density and distribution [9,10]. The precipitates observed in Mg-Y-Nd alloy have already been characterized in detail [10–12]. To achieve a more homogeneous microstructure, many studies performed heat treatments such as solution annealing or precipitation hardening on WE43 [13,14]. However, the correlation of bulk heat treatment and

surface morphology after electropolishing have not yet been investigated for Mg alloys.

In this study WE43 has been heat-treated with the aim to improve the quality of the electropolished surface by homogenizing and refining the microstructure.

## 2. Materials & methods

Cast WE43 (F) was used with the following composition: Y 4.8 wt%, Nd 2.1 wt% and Zr 0.1 wt% (LMpv, D-Dermbach). Before heat treatment, the ingot was cut into 25 × 10 × 10 mm blocks and wrapped in steel foil to prevent oxidation.

The specimens were first solution-treated (T4) at 540 °C for 4 h and quenched with water at 21 °C. Half of the solution-annealed samples were then immediately precipitation-hardened (T6) at 300 °C for 1 h and cooled in air. These parameters were chosen to keep the ageing time low, albeit finer precipitates could be produced at lower temperatures for longer periods.

For microstructural studies, WE43-F, WE43-T4 and WE43-T6 samples were ground with SiC paper up to P2500 and then polished with 3 μm and 1 μm diamond suspensions and with 0.03 μm colloidal silicon dioxide. Finally, the surfaces were etched with a solution of 20 ml acetic acid, 19 ml water, 1 ml nitric acid and 60 ml ethylene glycol.

Electropolishing was carried out at 21 °C in an electrolyte of

\* Corresponding author at: Biomaterials Laboratory, Ostbayerische Technische Hochschule (OTH) Regensburg, Seybothstraße 2, Regensburg 93053, Germany.

E-mail addresses: [jessica.kloiber@oth-regensburg.de](mailto:jessica.kloiber@oth-regensburg.de) (J. Kloiber), [ulrich.schultheiss@oth-regensburg.de](mailto:ulrich.schultheiss@oth-regensburg.de) (U. Schultheiß), [helga.hornberger@oth-regensburg.de](mailto:helga.hornberger@oth-regensburg.de) (H. Hornberger).

<https://doi.org/10.1016/j.matlet.2025.138821>

Received 27 March 2025; Received in revised form 19 May 2025; Accepted 25 May 2025

Available online 26 May 2025

0167-577X/© 2025 The Authors. Published by Elsevier B.V. This is an open access article under the CC BY license (<http://creativecommons.org/licenses/by/4.0/>).

phosphoric acid (85 vol%), ethanol (99 vol%) and deionized water in a ratio of 40:56:4 at a voltage of 2 V for 10 min [8]. Afterwards, the samples were rinsed with deionized water and ethanol (94 vol%) and dried with a blow-dryer.

Optical microscopy (OM) (BX51, Olympus) and the software ImageJ were used for microstructural analysis and confocal laser scanning microscopy (CLSM) (LEXT 4000, Olympus) for surface morphology analysis.

### 3. Results & discussion

Figs. 1, 2 and 3 show (a) the cross-sectional microstructures of WE43-F, WE43-T4 and WE43-T6 and (b) the surfaces of the three WE43 conditions after electropolishing, including (c) an exemplary height profile scan. Detailed analysis of primary grains and precipitates in the as-cast, T4 and T6 state and a roughness and surface defect investigation after electropolishing is presented in Fig. 4.

WE43-F is characterized by a typical cast microstructure of  $\alpha$ -Mg solid solution matrix with unevenly distributed coarse precipitates (Fig. 1a). Fig. 4a-b shows a mean grain size of 76  $\mu\text{m}$  and an area fraction of precipitates of 3.7 %, thereby the lengths of precipitates (the largest dimension) vary between 30–60  $\mu\text{m}$ . There are two different precipitates: The eutectic Mg-Nd-Y phase is visible in gray contrast along the grain boundaries and intermetallic particles in form of black spots are distributed non-uniformly at the grain boundaries or in clusters over several grains. Electropolishing led to a smooth surface with a roughness  $S_a$  of 0.08  $\mu\text{m}$  but a waviness  $S_z$  of 5  $\mu\text{m}$  (Fig. 4c). Fig. 1b shows on closer inspection the formation of spherical dents around the black intermetallic phases and wavy structures around the eutectic phases at the grain boundaries. The wavy structure in detail consists of large pits combined with spikes observed in the corresponding height profile (Fig. 1c). These findings indicate uneven surface processing during electropolishing due to precipitates within the as-cast material. Thereby the largest surface defect diameter of 48  $\mu\text{m}$  correlates with the average dimensions of the

eutectic phase (Fig. 4b + d). Beside precipitates, grain boundaries may also influence the quality of the electropolished surface. In some cases, grain boundaries were found to be visible after electropolishing, probably caused by slightly too high voltages during processing, which should be studied in future.

T4 treatment caused a tenfold increase of the primary grain size but most of the precipitates to dissolve into the matrix (Figs. 2a and 4a). The area fraction of precipitates decreased to 0.6 % (Fig. 4b). The eutectic phase at the grain boundaries has completely disappeared. The black particles have been reduced in their accumulation but not dissolved. After electropolishing, the WE43-T4 surface shows also remaining small black particles, which did not produce defects in form of dents (Fig. 2b). The CLSM measurement revealed a uniform, mirror-smooth and largely structureless surface profile (Fig. 2c) with values of 0.01  $\mu\text{m}$  for  $S_a$  and less than 2  $\mu\text{m}$  for  $S_z$  (Fig. 4c).

The precipitation hardening did not lead to further grain growth compared with T4, but the area fraction of precipitates increased to 7.9 % (Figs. 3a and 4a-b). T6 produced a uniform microstructure with a dense distribution of fine scale needle-shaped precipitates of the previously dissolved secondary phase, which are now located inside the  $\alpha$ -Mg grains. Fig. 3b shows the electropolished surface of WE43-T6. Despite the remaining black particles and the increased volume fraction of precipitates, the surface has no defects in form of pits or dents (Fig. 3c). The roughness  $S_a$  is 0.02  $\mu\text{m}$  and waviness  $S_z$  less than 2  $\mu\text{m}$  (Fig. 4c). This refinement means that there are no more areas in the microstructure that are subject to increased removal during electropolishing, thus enabling uniform electrochemical treatment.

### 4. Conclusion

This study shows that microstructural modification of precipitations can have a significant impact on the quality of electropolished surfaces of Mg material. A nearly homogenized WE43-T4 microstructure correlates with lower roughness and less defects of the electropolished

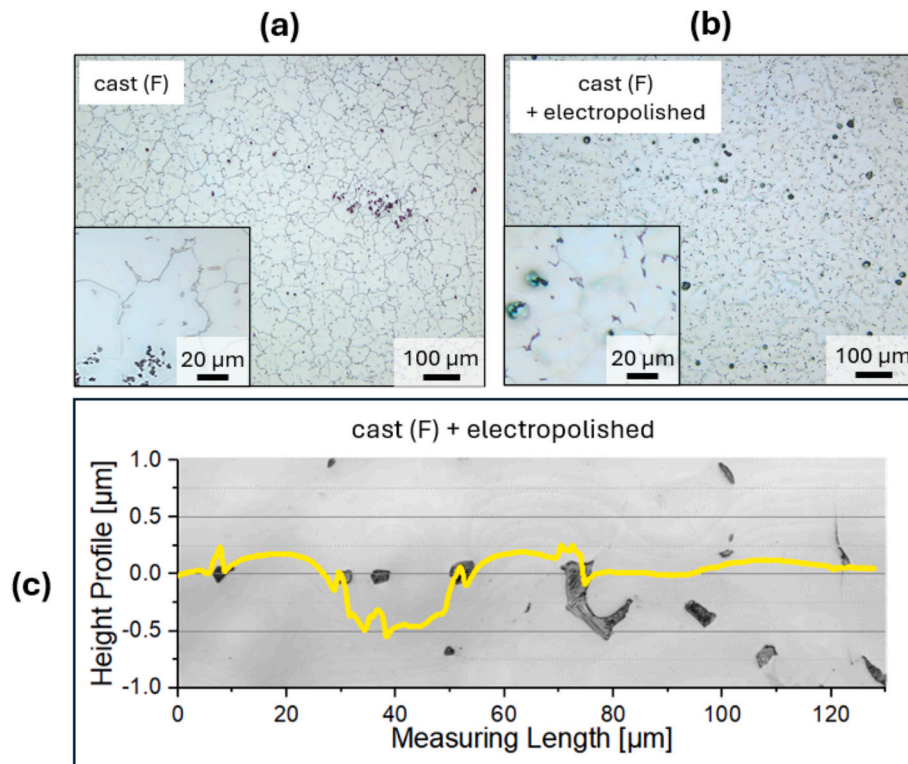


Fig. 1. OM of (a) the microstructure of the as-cast WE43-F and (b) its surface after electropolishing. CLSM revealed (c) the detailed surface morphology, the more inhomogeneous the microstructure, the higher the proportion of defects on the electropolished surface.

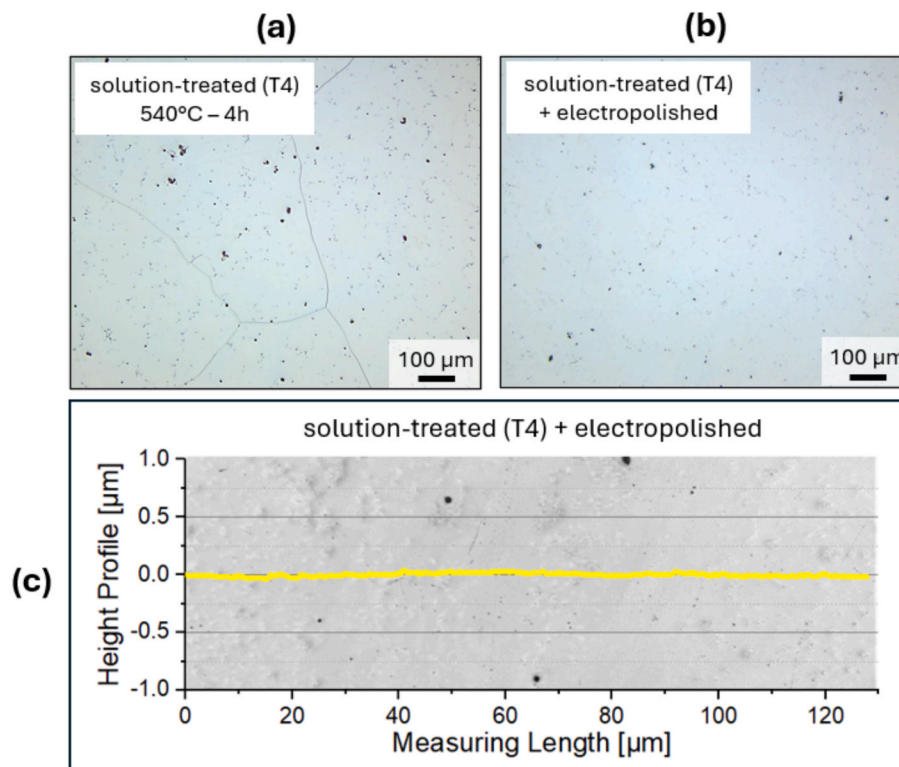


Fig. 2. OM of (a) the WE43-T4 microstructure after solution annealing and (b) its surface after electropolishing. CLSM revealed (c) the detailed surface morphology, the homogenization of the microstructure leads to a mirror-smooth and defect-free electropolished surface.

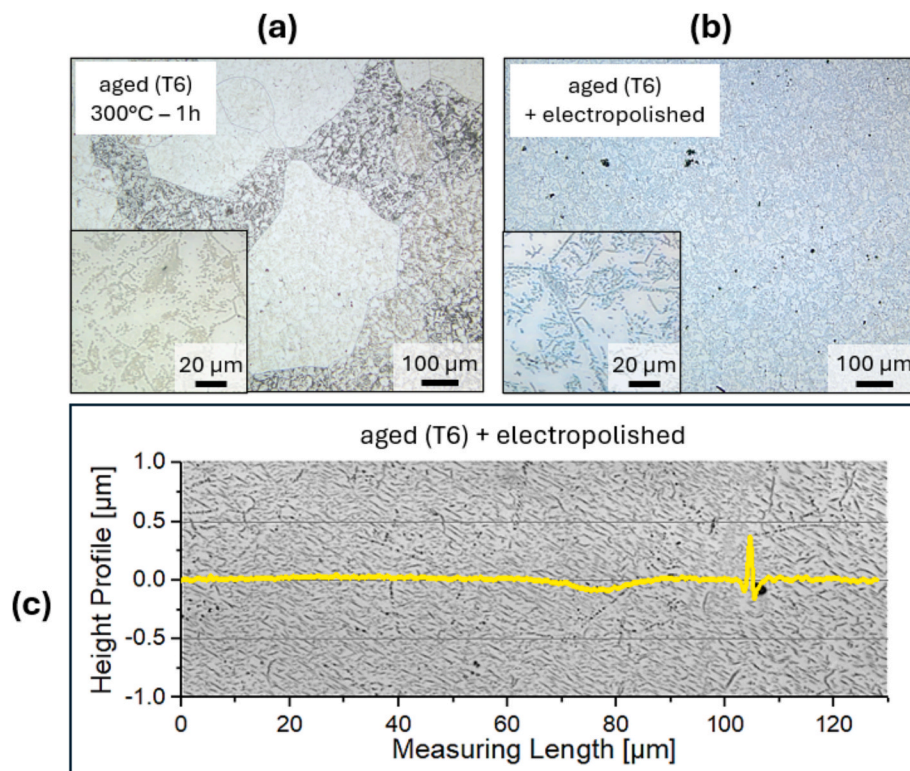
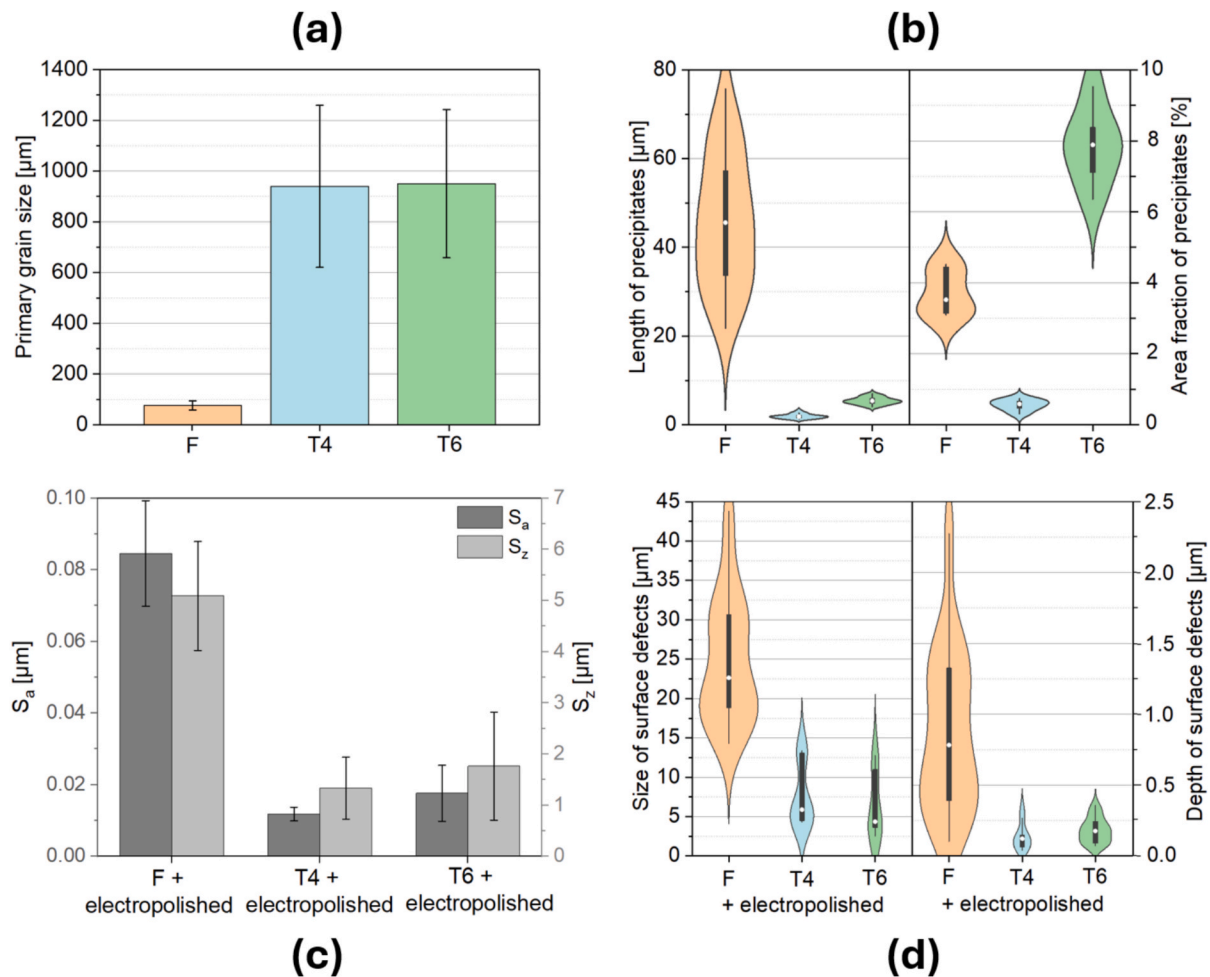


Fig. 3. OM of (a) the WE43-T6 microstructure after aging and (b) its surface after electropolishing. CLSM revealed (c) the detailed surface morphology, the microstructural refinement enables uniform material removal during electropolishing.



**Fig. 4.** (a) Mean grain size, (b) length and area fraction of precipitations of WE43 after different heat treatments and (c) surface roughness and (d) size and depth of surface defects after subsequently electropolishing. No or finely distributed secondary phases led to defect-reduced and smooth electropolished surfaces.

surfaces, approx.  $0.02 \mu\text{m}$  for  $S_a$  and less than  $2 \mu\text{m}$  for  $S_z$  compared to  $0.08 \mu\text{m}$  and  $5 \mu\text{m}$  for WE43-F. WE43-T6 shows that precipitates can also enable a uniformly electropolished surface. Thereby, the quantity of precipitates was not decisive for high surface quality but the size and morphology of the secondary phases. Precipitate sizes of  $30\text{--}60 \mu\text{m}$  produced surface defects in a similar size range but needle lengths of about  $5 \mu\text{m}$  could be neglected, the electropolished surface quality appeared the same as for solid solution matrix.

#### CRediT authorship contribution statement

**Jessica Kloiber:** Writing – original draft, Visualization, Validation, Methodology, Investigation, Data curation, Conceptualization. **Ulrich Schultheiß:** Writing – review & editing, Methodology, Conceptualization. **Helga Hornberger:** Writing – review & editing, Supervision, Resources, Project administration, Methodology, Funding acquisition, Conceptualization.

#### Declaration of competing interest

The authors declare that they have no known competing financial interests or personal relationships that could have appeared to influence the work reported in this paper.

#### Acknowledgements

The authors gratefully thank Regensburg Center of Biomedical

Engineering for providing laboratory consumables. They thank Studienstiftung des deutschen Volkes and Elitenetzwerk Bayern for financial support of J. Kloiber.

#### Data availability

Data will be made available on request.

#### References

- [1] Y. Li, A. Zhang, C. Li, H. Xie, B. Jiang, Z. Dong, P. Jin, F. Pan, Recent advances of high strength Mg-RE alloys: alloy development, forming and application, *J. Mater. Res. Technol.* 26 (2023) 2919–2940, <https://doi.org/10.1016/j.jmrt.2023.08.055>.
- [2] D. Liu, D. Yang, X. Li, S. Hu, Mechanical properties, corrosion resistance and biocompatibilities of degradable Mg-RE alloys: a review, *J. Mater. Res. Technol.* 8 (2019) 1538–1549, <https://doi.org/10.1016/j.jmrt.2018.08.003>.
- [3] C.C. Zhao, W.T. Ouyang, M. Wen, C. Yang, D.K. Xu, Y.F. Zheng, T.F. Xi, L.Y. Sheng, Optimizing corrosion resistance of the Mg-4Zn-0.5Y-0.5Nd alloy by regulation of secondary phase and grain structure, *J. Mater. Res. Technol.* 35 (2025) 435–450, <https://doi.org/10.1016/j.jmrt.2025.01.062>.
- [4] C. Zhao, M. Wen, Q. Wang, W. Ouyang, D. Xu, Z. Jia, Y. Zheng, T. Xi, L. Sheng, Tailoring the corrosion resistance and biological performance of Mg-Zn-Y-Nd bioimplants with multiphase, pore-sealed cerium-doped ceramic coatings via facile one-pot plasma electrolytic oxidation, *J. Mater. Sci. Technol.* 230 (2025) 60–79, <https://doi.org/10.1016/j.jmst.2025.01.016>.
- [5] T. Zhang, W. Wang, J. Liu, L. Wang, Y. Tang, K. Wang, A review on magnesium alloys for biomedical applications, *Front. Bioeng. Biotechnol.* 10 (2022) 953344, <https://doi.org/10.3389/fbioe.2022.953344>.
- [6] K.-P. Liu, J.-L. You, S.-Y. Jian, Y.-H. Chang, C.C. Tseng, M.-D. Ger, Effect of electropolishing parameters of WE43 magnesium alloy on corrosion resistance of artificial plasma, *J. Mater. Res. Technol.* 26 (2023) 4989–5000, <https://doi.org/10.1016/j.jmrt.2023.08.189>.

- [7] J. Kloiber, U. Schultheiß, L. Sotelo, G. Sarau, S. Christiansen, S. Gavras, N. Hort, H. Hornberger, Corrosion behaviour of electropolished magnesium materials, *Mater. Today Commun.* 38 (2024) 107983, <https://doi.org/10.1016/j.mtcomm.2023.107983>.
- [8] J. Kloiber, V. Anetsberger, U. Schultheiß, H. Hornberger, High quality surfaces of magnesium alloy AZ31 by adjusting appropriate electropolishing parameters, *Electrochim. Acta* 513 (2025) 145547, <https://doi.org/10.1016/j.electacta.2024.145547>.
- [9] Y. Lu, A.R. Bradshaw, Y.L. Chiu, I.P. Jones, Effects of secondary phase and grain size on the corrosion of biodegradable Mg-Zn-Ca alloys, *Mater. Sci. Eng. C Mater. Biol. Appl.* 48 (2015) 480–486, <https://doi.org/10.1016/j.msec.2014.12.049>.
- [10] D. Dvorský, J. Kubásek, K. Hosová, M. Čavojský, D. Vojtěch, Microstructure, mechanical, corrosion, and ignition properties of WE43 alloy prepared by different processes, *Metals* 11 (2021) 728, <https://doi.org/10.3390/met11050728>.
- [11] D. Tolnai, C.L. Mendis, A. Stark, G. Szakács, B. Wiese, K.U. Kainer, N. Hort, In situ synchrotron diffraction of the solidification of Mg4Y3Nd, *Mater. Lett.* 102–103 (2013) 62–64, <https://doi.org/10.1016/j.matlet.2013.03.110>.
- [12] C. Xiang, N. Gupta, P. Coelho, K. Cho, Effect of microstructure on tensile and compressive behavior of WE43 alloy in as cast and heat treated conditions, *Mater. Sci. Eng. A* 710 (2018) 74–85, <https://doi.org/10.1016/j.msea.2017.10.084>.
- [13] M.M. Zerankeshi, R. Alizadeh, E. Gerashi, M. Asadollahi, T.G. Langdon, Effects of heat treatment on the corrosion behavior and mechanical properties of biodegradable Mg alloys, *J. Magnes. Alloy* 10 (2022) 1737–1785, <https://doi.org/10.1016/j.jma.2022.04.010>.
- [14] P. Maier, R. Peters, C.L. Mendis, S. Müller, N. Hort, Influence of precipitation hardening in Mg-Y-Nd on mechanical and corrosion properties, *JOM* 68 (2016) 1183–1190, <https://doi.org/10.1007/s11837-015-1762-4>.